

Supporting information

Experimental and Simulation Insights into Local Structure and Luminescence Evolution in Eu³⁺-Doped Nanocrystals under High Pressure

Sheng Mei[†], Yu Guo[†], Xiaohuan Lin[‡], Hao Dong[†], Ling-Dong Sun^{†}, Kuo Li^{*‡}, Chun-Hua Yan^{*†,§}*

[†]Beijing National Laboratory for Molecular Sciences, State Key Laboratory of Rare Earth Materials Chemistry and Applications, PKU-HKU Joint Laboratory in Rare Earth Materials and Bioinorganic Chemistry, College of Chemistry and Molecular Engineering, Peking University, Beijing 100871, China

[‡]Center for High Pressure Science and Technology Advanced Research, Beijing 100094, China

[§]College of Chemistry and Chemical Engineering, Lanzhou University, Lanzhou 730000, China

**Corresponding authors: sun@pku.edu.cn; likuo@hpstar.ac.cn; yan@pku.edu.cn.*

Experimental Section

Materials

RE oxides (RE = Gd, Eu; China Rare Earth Online Co., Ltd), Oleic acid (OA; >90%, Sigma-Aldrich), oleylamine (OM; >80%, J&K), 1-octadecene (ODE; >90%, J&K), trifluoroacetic acid (99%, Acros), trifluoroacetic acid sodium salt (99%, Acros), RE chloride hexahydrate ($\text{GdCl}_3 \cdot 6\text{H}_2\text{O}$, $\text{EuCl}_3 \cdot 6\text{H}_2\text{O}$; 99.9%, Aladdin), ethanol (AR), cyclohexane (AR). Analytical grade NaBF_4 , trisodium citrate (Na_3Cit), and NaOH were purchased from Sinopharm Chemical Reagent Co., Ltd. All chemicals were used as received without further purification. $\text{RE}(\text{CF}_3\text{COO})_3$ (RE = Gd, Eu) were prepared from the corresponding RE oxides and trifluoroacetic acid. Water used in all experiments was obtained using a Milli-Q water system.

Synthesis of 10 nm $\beta\text{-NaGdF}_4\text{:Eu}^{3+}$ NCs

The preparation of 10 nm NCs involved the synthesis of α -phase NCs, followed by a phase transition process. Typically, a given amount of CF_3COONa (1.00 mmol) and $\text{Gd}(\text{CF}_3\text{COO})_3$ (0.95 mmol) and $\text{Eu}(\text{CF}_3\text{COO})_3$ (0.05 mmol) was added into a mixture of OA, OM and ODE (10 mmol: 10mmol: 20 mmol) in a three-necked flask (100 mL) at room temperature. Then the slurry was heated to 120°C to remove water and oxygen with vigorous magnetic stirring under vacuum. The solution was heated to 310°C and kept for 15 min under N_2 atmosphere. After cooling to room temperature, an excess amount of ethanol was added into the solution to precipitate and collect the α -phase NCs by centrifugation. The α -phase NCs was dispersed in 10 mL of cyclohexane. After that, 5 mL as-prepared α -phase NCs colloidal solution was redispersed in a mixture of OA and ODE (20 mmol: 20 mmol), additional $\text{Gd}(\text{CF}_3\text{COO})_3$ (0.475 mmol), $\text{Eu}(\text{CF}_3\text{COO})_3$ (0.025 mmol) and CF_3COONa (0.50 mmol) were also added. The slurry was heated to 110°C to remove cyclohexane, water, and oxygen with vigorous magnetic stirring under vacuum. Then the solution was heated to 310°C and kept for 30 min under N_2 atmosphere. Upon cooling to room temperature, $\beta\text{-NaGdF}_4\text{:Eu}^{3+}$ NCs were separated by centrifugation after adding an excess amount of ethanol. The product was washed with ethanol three times to remove excess OA ligands, and dried in vacuum oven at 80°C for 12 h.

Synthesis of $\beta\text{-NaGdF}_4\text{:Eu}^{3+}$ NCs of other sizes

The preparation of 40 nm NCs was through the epitaxial growth of shell layer on 10 nm NCs. 0.25 mmol of 10 nm NCs was redispersed in a mixture of OA and ODE (20 mmol: 20 mmol), along with $\text{RE}(\text{CF}_3\text{COO})_3$ (RE = Gd, Eu, 1mmol) of the same proportion and CF_3COONa (1 mmol). The slurry was heated to 110°C to remove cyclohexane, water, and oxygen with vigorous magnetic stirring under vacuum. Then the solution was heated to 310°C and kept for 30 min under N_2 atmosphere. Upon cooling to room temperature, $\beta\text{-NaGdF}_4\text{:Eu}^{3+}$ NCs were isolated by centrifugation after adding an excess amount of ethanol. The as-prepared NCs were used as the core to repeat the procedure to get 40 nm NCs.

The 250 nm NCs were prepared with a modified hydrothermal method.^[S1] 0.95 mmol $\text{GdCl}_3 \cdot 6\text{H}_2\text{O}$ and 0.05 mmol $\text{EuCl}_3 \cdot 6\text{H}_2\text{O}$ were dissolved in 5mL H_2O , and the solution was mixed with 10 mL of 0.1M Na_3Cit solution to form RE-Cit^{3-} complex. After vigorous stirring, 3.125 mmol of NaBF_4 was added into the above solution. The pH of the mixture was adjusted to 7 by adding 1 M NaOH . The obtained solution was then transferred into a Teflon-lined autoclave and maintained at 190°C for 24 h. The 500 nm NCs were prepared under the same condition except that the reaction temperature was

elevated to 200°C.

High-pressure measurements

High-pressure experiments were carried out by using a diamond anvil cell (DAC)^[S2] with 400 μm diameter culets. Samples were loaded into 160 μm diameter holes drilled in T301 stainless steel gaskets, which were preindented from 250 μm thick to 50 μm . Small ruby balls were inserted into the sample compartment for *in situ* pressure calibration, based on the R1 ruby fluorescence method.^[S3] The *in situ* PL measurements under high pressure were performed on a Renishaw inVia spectrometer in the PL mode. The 488 nm line of an Ar^+ laser with a spot size of 20 μm and a power of 0.052 mW was used as the excitation source. The angle dispersive X-ray diffraction measurements up to 35.9 GPa were conducted at 4W2 beamline of the Beijing Synchrotron Radiation Facility (BSRF). The wavelength of the incident beam was 0.6199 Å, and the beam size was 35 μm \times 12 μm . Neon was used as the pressure-transmitting medium. The two-dimensional XRD data reduction was performed using the Dioptas program.^[S4]

TEM characterizations

TEM characterizations were performed on a JEOL 2100 operated at 200 kV. For synthesized NCs, the sample in solution (~ 10 μL) was dropped onto a 300-mesh copper TEM grid and dried at ambient condition. For the pressurized samples, the specimens were collected and redispersed in solution before TEM measurements.

DFT calculations

The Density Functional Theory (DFT) calculations were carried out with the Vienna ab initio simulation package (VASP)^[S5]. The exchange-correlation energy functional was described with the Perdew-Burke-Ernzerhof (PBE)^[S6] generalized gradient approximation (GGA). The core atoms were presented by projector augmented wave (PAW) pseudopotentials^[S7]. The $3 \times 2 \times 1$ $\beta\text{-NaGdF}_4$ supercell was built with one Gd ion replaced by the Eu ion, for which $3 \times 3 \times 5$ Monkhorst-Pack k-point sampling^[S8] was used. The kinetic cutoff energy was 500 eV. Different Hubbard U parameters were used for Ln 4f orbitals and F 2p orbitals, that is, 9 and 2.7 eV of U were imposed on the two types of Gd ions, 4.36, 4.25 and 4.2 eV of U were imposed on three kinds of F ions and 7.8 eV of U was on the Eu ion.^[S9] Each structure was relaxed until the residual force was less than 0.02 eV/Å.

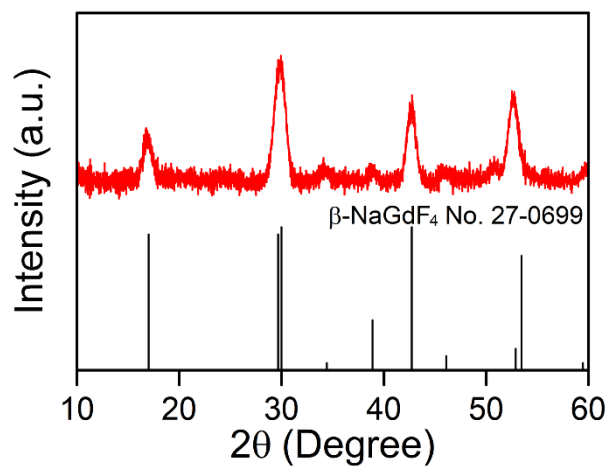


Figure S1. XRD pattern of 10 nm β -NaGdF₄:Eu³⁺ NCs under ambient condition.

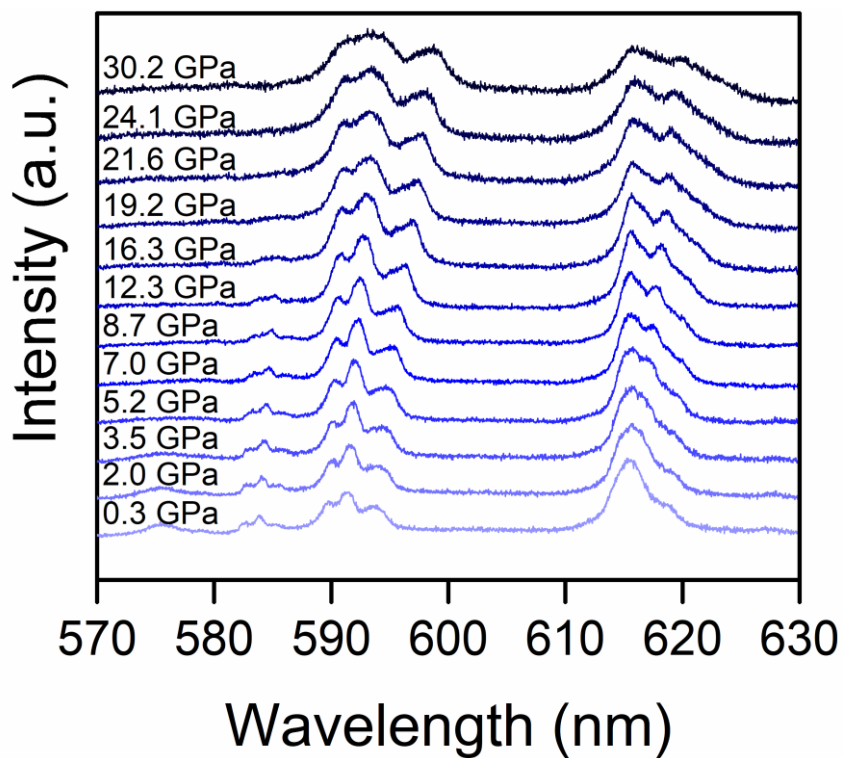


Figure S2. Normalized emission spectra of 10 nm β -NaGdF₄:Eu³⁺ NCs during the decompression process.

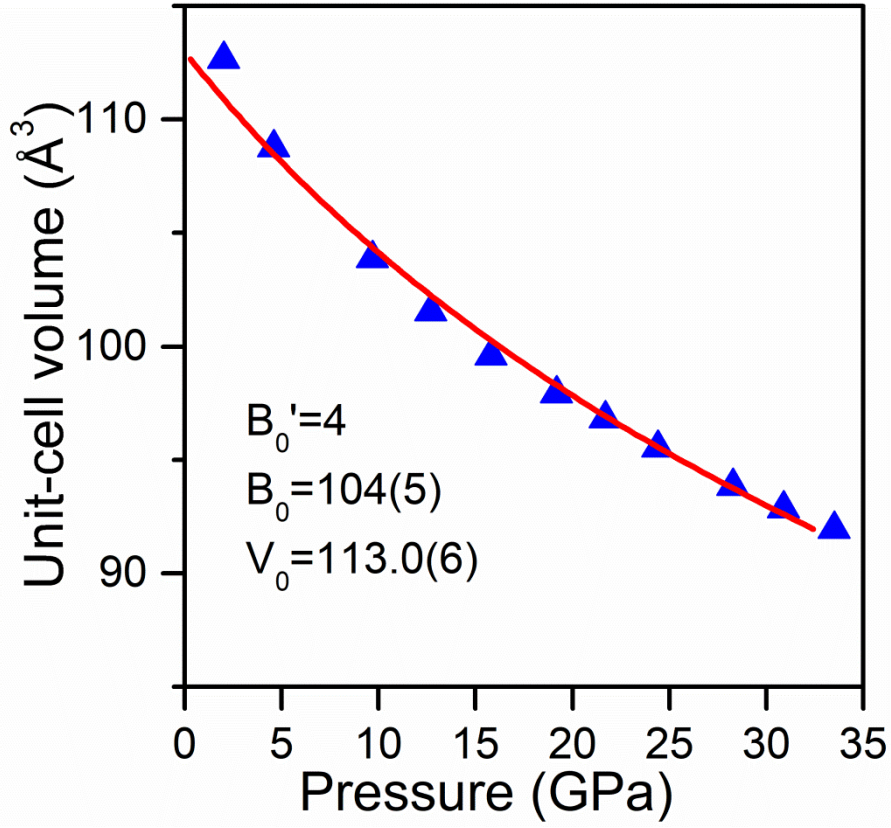


Figure S3. High-pressure evolution of unit-cell volume and fitted curve of 10 nm β -NaGdF₄:Eu³⁺ NCs. The P–V data is fitted based on the third-order Birch–Murnaghan equation of state $P = \frac{3}{4}B_0[(V_0/V)^{7/3} - (V_0/V)^{5/3}] \times \{1 + \frac{3}{4}(B_0' - 4)[(V_0/V)^{2/3}]\}$, where V_0 is the volume at ambient pressure, B_0 is the bulk modulus at ambient pressure, and B_0' is a parameter for pressure derivative. B_0' is fixed at 4 for our fitting. The bulk modulus $B_0 = 104(5)$ GPa for 10 nm β -NaGdF₄:Eu³⁺ NCs.

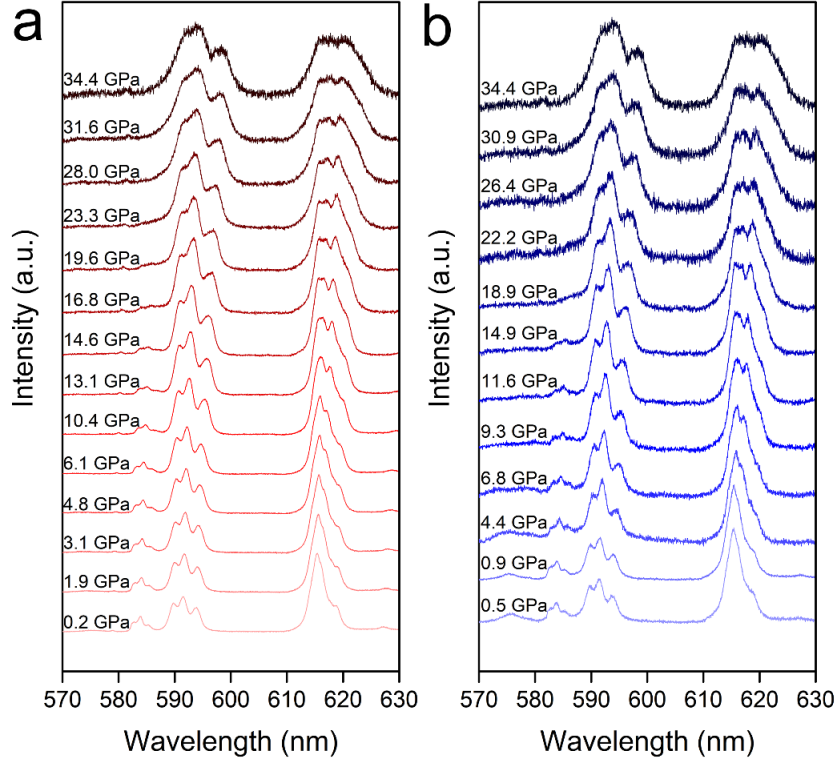


Figure S4. Normalized emission spectra of 40 nm β -NaGdF₄:Eu³⁺ NCs during the compression (a) and decompression (b) cycle.

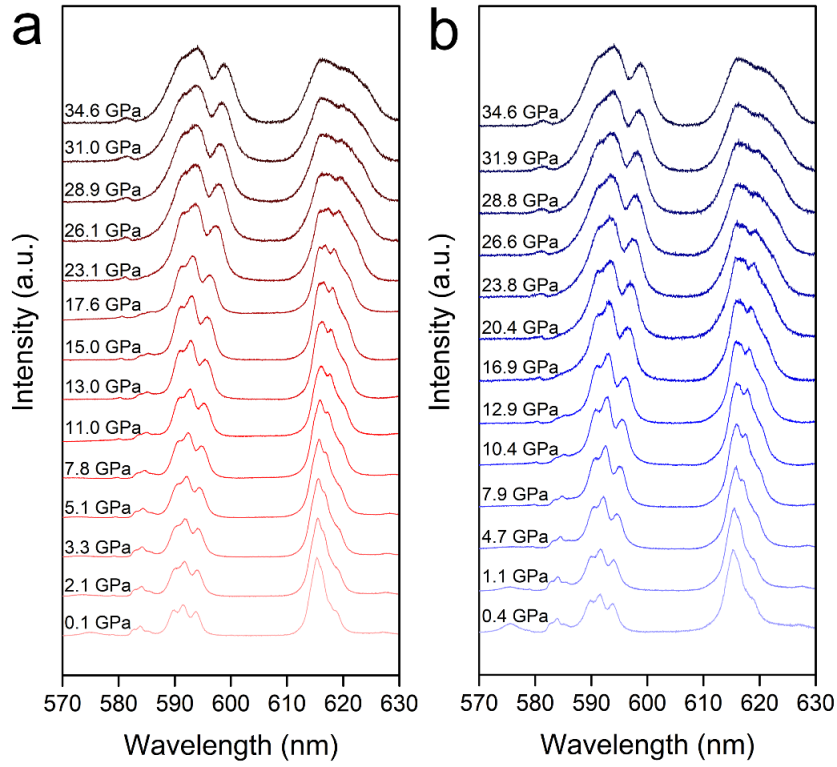


Figure S5. Normalized emission spectra of 250 nm β -NaGdF₄:Eu³⁺ NCs during the compression (a) and decompression (b) cycle.

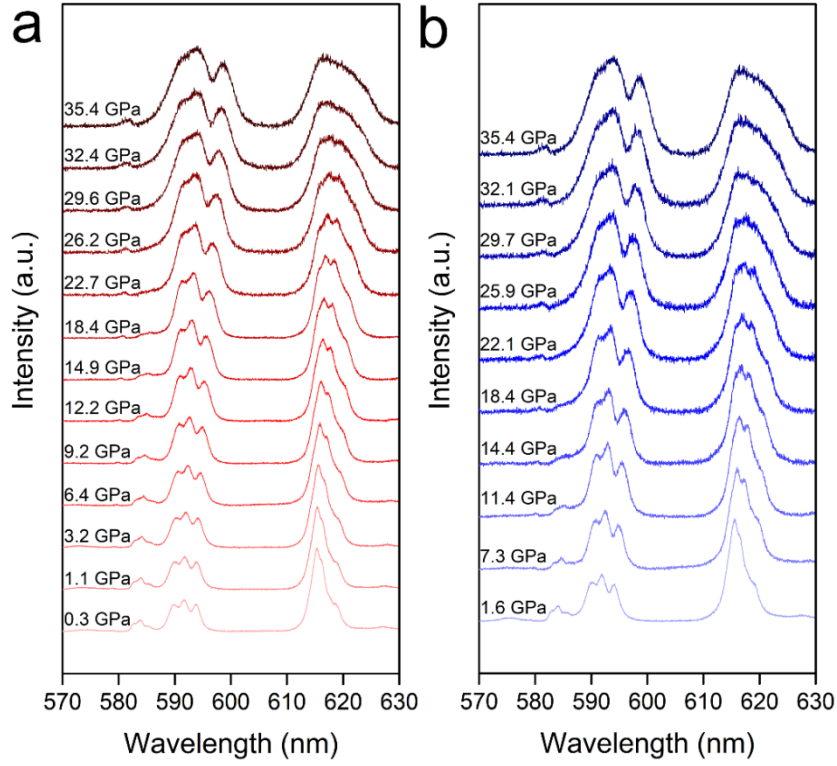


Figure S6. Normalized emission spectra of 500 nm β -NaGdF₄:Eu³⁺ NCs during the compression (a) and decompression (b) cycle.

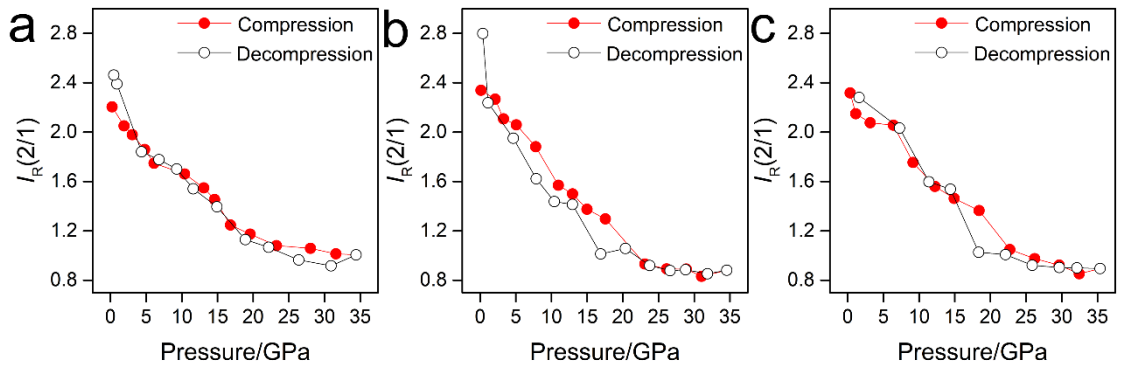


Figure S7. Variation of intensity ratios $I_R(2/1)$ of β -NaGdF₄:Eu³⁺ NCs with different sizes during the compression (solid circles) and decompression (open circles) cycle, (a) 40 nm NCs, (b) 250 nm NCs, (c) 500 nm NCs.

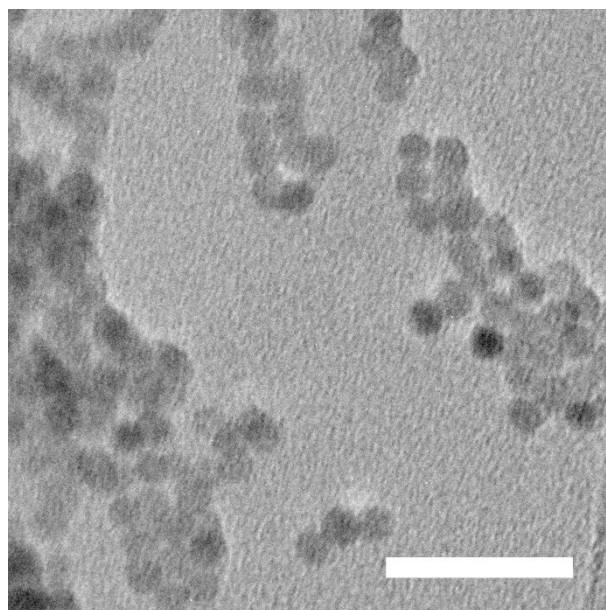


Figure S8. TEM image of 10 nm β -NaGdF₄:Eu³⁺ NCs after the compression-decompression cycle. Scale bar is 50 nm.

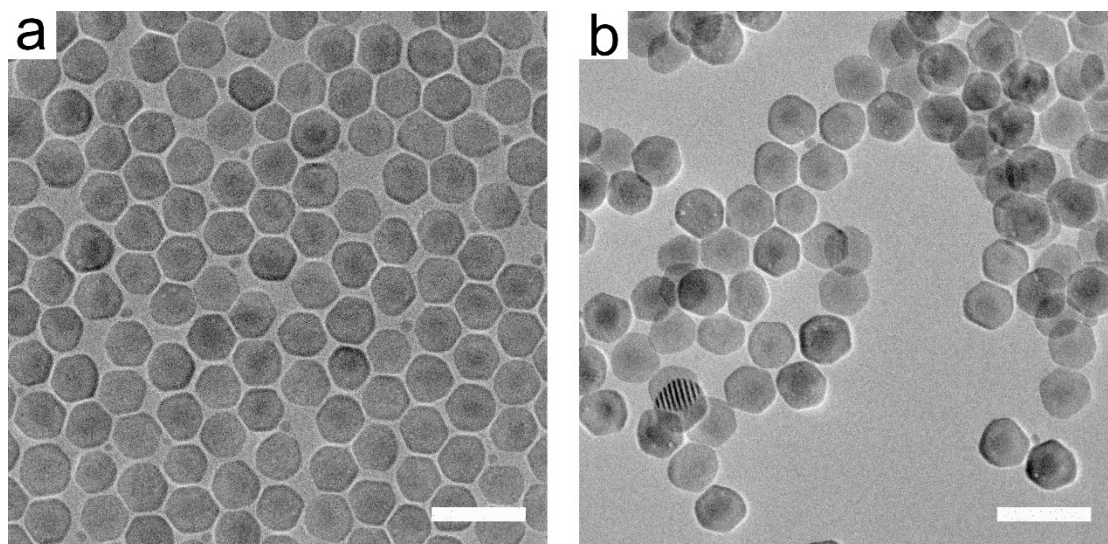


Figure S9. TEM image of 40 nm β -NaGdF₄:Eu³⁺ NCs before (a) and after (b) the compression-decompression cycle. Scale bar is 100 nm.

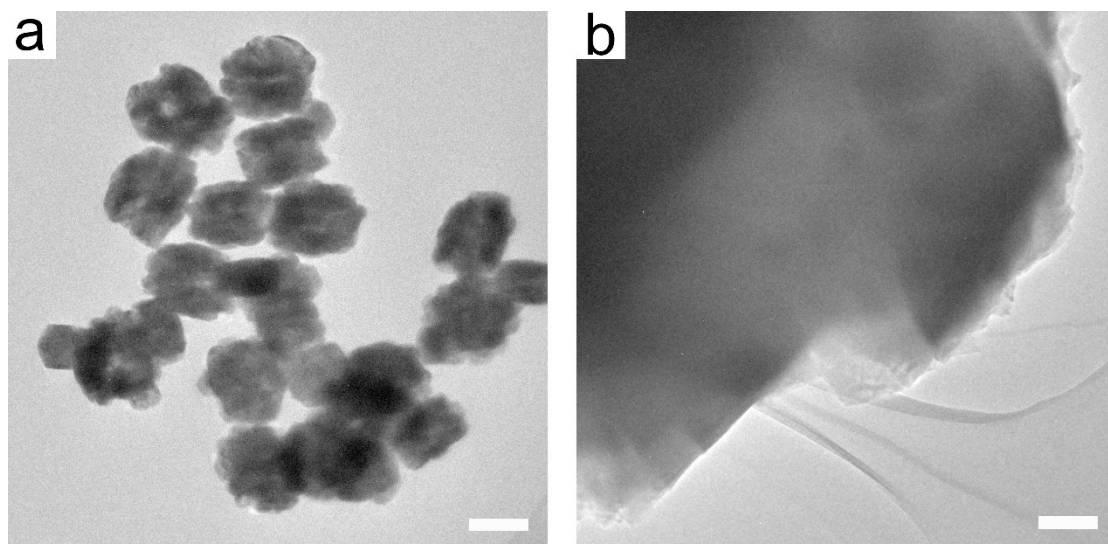


Figure S10. TEM image of 250 nm β -NaGdF₄:Eu³⁺ NCs before (a) and after (b) the compression-decompression cycle. Scale bar is 200 nm.

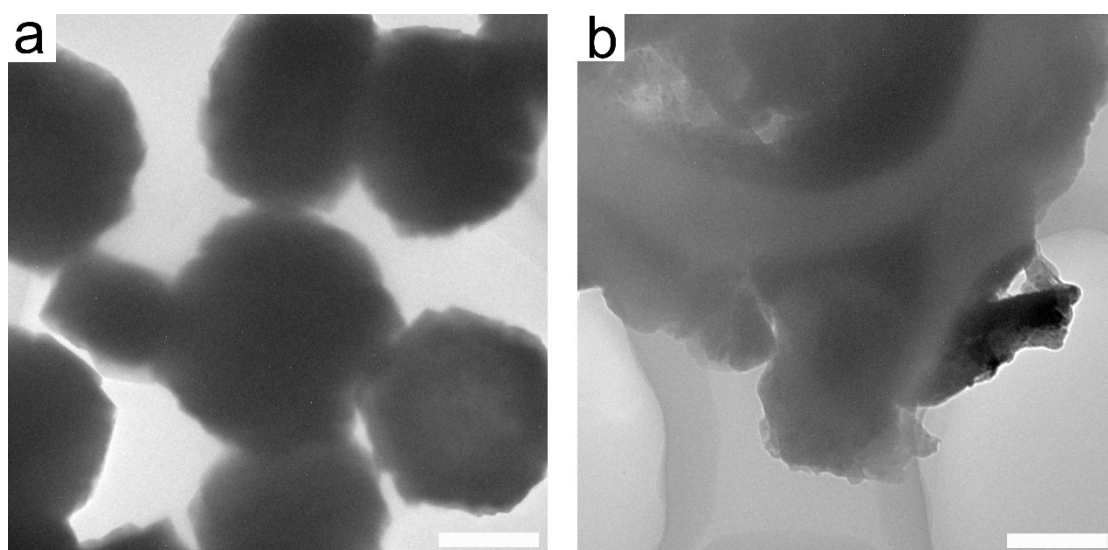


Figure S11. TEM image of 500 nm β -NaGdF₄:Eu³⁺ NCs before (a) and after (b) the compression-decompression cycle. Scale bar is 500 nm.

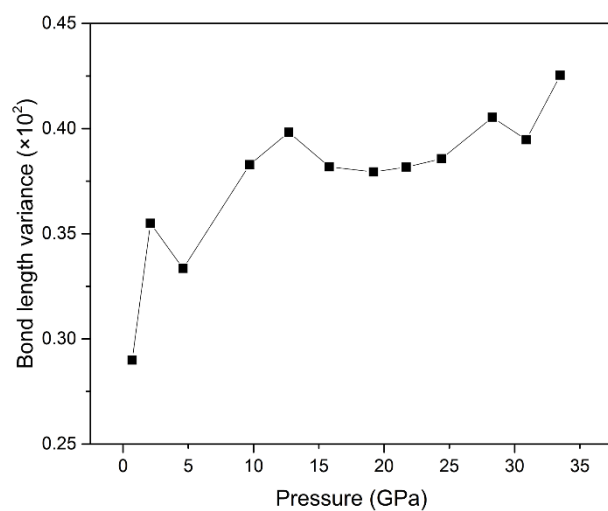


Figure S12. The variance of Gd-F bond length under different pressures.

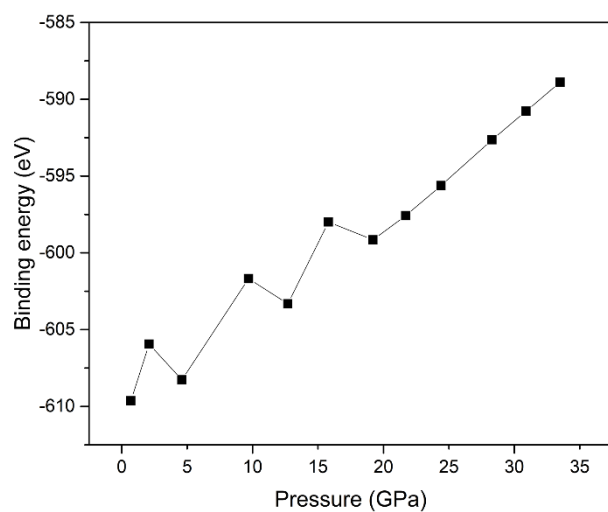


Figure S13. Variation of binding energies of β -NaGdF₄ under different pressures.

Table S1. Refined lattice parameters of β -NaGdF₄:Eu³⁺ NCs obtained from XRD under different pressures

Pressure (GPa)	<i>a</i> (Å)	<i>c</i> (Å)	<i>V</i> (Å ³)
0.7	6.042(2)	3.646(2)	115.3(2)
2.1	5.991(3)	3.624(2)	112.6(2)
4.6	5.927(2)	3.575(2)	108.8(2)
9.7	5.823(2)	3.538(1)	103.9(1)
12.7	5.776(2)	3.514(2)	101.5(2)
15.8	5.743(2)	3.486(2)	99.6(2)
19.2	5.706(2)	3.473(2)	97.9(2)
21.7	5.681(2)	3.464(2)	96.8(1)
24.4	5.657(2)	3.448(2)	95.5(1)
28.3	5.618(2)	3.433(2)	93.8(1)
30.9	5.598(2)	3.422(2)	92.9(1)
33.5	5.573(2)	3.419(2)	92.0(1)

Table S2. The optimized Gd-F bond lengths and surface intersection angles under different pressures

Pressure (GPa)	^a C1 (Å)	C2 (Å)	C3 (Å)	T1 (Å)	T2 (Å)	T3 (Å)	B1 (Å)	B2 (Å)	B3 (Å)	Variance (x 10 ²)	Angle (°)
0.7	2.300	2.302	2.304	2.398	2.383	2.389	2.423	2.420	2.422	0.290	6.39
2.1	2.287	2.283	2.285	2.388	2.373	2.373	2.408	2.427	2.420	0.355	5.91
4.6	2.270	2.273	2.269	2.375	2.350	2.354	2.390	2.403	2.406	0.333	4.99
9.7	2.242	2.241	2.241	2.345	2.329	2.333	2.378	2.380	2.385	0.383	3.27
12.7	2.231	2.229	2.229	2.335	2.321	2.324	2.369	2.371	2.376	0.398	2.46
15.8	2.223	2.221	2.223	2.324	2.309	2.310	2.358	2.363	2.366	0.382	2.02
19.2	2.215	2.214	2.214	2.313	2.299	2.301	2.351	2.353	2.359	0.379	1.74
21.7	2.210	2.209	2.209	2.304	2.292	2.296	2.347	2.350	2.354	0.382	1.63
24.4	2.205	2.202	2.202	2.300	2.284	2.286	2.338	2.347	2.349	0.386	1.44
28.3	2.193	2.191	2.194	2.290	2.275	2.277	2.338	2.338	2.339	0.405	1.02
30.9	2.189	2.188	2.188	2.282	2.266	2.272	2.331	2.333	2.333	0.395	0.59
33.5	2.183	2.180	2.180	2.276	2.262	2.266	2.327	2.333	2.332	0.425	0.72

^aC1-C3, T1-T3 and B1-B3 denote the lengths of Gd-F bonds pointing to the three caps and the top and bottom surfaces of the trigonal prism, respectively.

REFERENCES

- [S1] He, F.; Yang, P.; Wang, D.; Niu, N.; Gai, S.; Li, X. Self-assembled β -NaGdF₄ microcrystals: hydrothermal synthesis, morphology evolution, and luminescence properties. *Inorg. Chem.* **2011**, *50*, 4116-4124.
- [S2] Mao, H. K.; Bell, P. M. The ultrahigh-pressure diamond cell: Design applications for electrical measurements of mineral samples at 1.2 MBar. *Year Book-Carnegie Inst. Washington* **1976**, *75*, 824-827.
- [S3] Mao, H. K.; Xu, J.; Bell, P. M. Calibration of the ruby pressure gauge to 800 kbar under quasi-hydrostatic conditions. *J. Geophys. Res.-Sol. Ea.* **1986**, *91*, 4673-4676.
- [S4] Prescher, C.; Prakapenka, V. B. DIOPTAS: a program for reduction of two-dimensional X-ray diffraction data and data exploration. *High Pressure Res.* **2015**, *35*, 223-230.
- [S5] Hafner, J. Ab - initio simulations of materials using VASP: Density - functional theory and beyond. *J. Comput. Chem.* **2008**, *29*, 2044-2078.
- [S6] Perdew, J. P.; Burke, K.; Ernzerhof, M. Perdew, burke, and ernzerhof reply. *Phys. Rev. Lett.* **1998**, *80*, 891.
- [S7] Blöchl, P. E. Projector augmented-wave method. *Phys. Rev. B* **1994**, *50*, 17953.
- [S8] Monkhorst, H. J.; Pack, J. D. Special points for Brillouin-zone integrations. *Phys. Rev. B* **1976**, *13*, 5188.
- [S9] Huang, B.; Dong, H.; Wong, K.-L.; Sun, L.-D.; Yan, C.-H. Fundamental view of electronic structures of β -NaYF₄, β -NaGdF₄, and β -NaLuF₄. *J. Phys. Chem. C* **2016**, *120*, 18858-18870.